

Article

PM₁₀ and PM_{2.5} Qualitative Source Apportionment Using Selective Wind Direction Sampling in a Port-Industrial Area in Civitavecchia, Italy

Maria Eleonora Soggiu ¹, Marco Inglese ¹, Roberta Valentina Gagliardi ¹, Gaetano Settimo ¹, Giovanni Marsili ², Ivan Notardonato ³ and Pasquale Avino ^{3,*}

¹ Italian Institute of Health, Viale Regina Elena 299, I-00185 Rome, Italy; eleonora.soggiu@iss.it (M.E.S.); marco.inglessis@iss.it (M.I.); roberta.gagliardi@iss.it (R.V.G.); gaetano.settimo@iss.it (G.S.)

² Consorzio per la Gestione dell'Osservatorio Ambientale, Via delle Saline 18, Tarquinia, I-01100 Viterbo, Italy; marsiligianni@gmail.com

³ Department of Agriculture, Environmental and Food Sciences, University of Molise, via F. De Sanctis, I-86100 Campobasso, Italy; notardonatoivan@hotmail.com

* Correspondence: avino@unimol.it; Tel.: +39-06-0874-404631

Received: 30 November 2019; Accepted: 7 January 2020; Published: 13 January 2020



Abstract: The possibility to discriminate between different emission sources and between natural and anthropogenic contributions is a key issue for planning efficient air pollution reduction and mitigation strategies. Moreover, the knowledge of the particulate matter (PM) chemical composition for the different size fractions is recognized as increasingly important, in particular with respect to health effects of exposed population. This study is focused on the characterization of PM₁₀ and PM_{2.5} main sources located in the Civitavecchia harbor-industrial area (Central Italy), namely a large coal-fired power plant, a natural gas power plant, the harbor area, the vehicular traffic (due to both the local traffic and the highway crossing the area) and small industrial activities. The approach was based on PM₁₀/PM_{2.5} samples monthly collected for one year and a further relative chemical characterization of organic and inorganic fractions. Wind-select sensors, allowing a selective PM₁₀ and PM_{2.5} sampling downwind to specific emission sources, were used for the overall sampling. This methodology manages to explain specific emission patterns and to assess the concentration levels of the micro pollutants emitted by local sources and particularly toxic for health. A descriptive statistical analysis of data was performed, also verifying the occurrence of legislative threshold exceedances. Moreover, in order to highlight the contribution of specific sources, the differences in the measured micro pollutants concentrations between wind directions, PM size fractions and sampling sites have been investigated, as well as the seasonal trends of pollutants concentrations. These results allow to highlight that the applied methodology represents a valid support in source apportionment studies.

Keywords: PM₁₀; PM_{2.5}; wind select-sampling device; harbor; chemical composition; PAHs; metals; PCCD/F; source apportionment

1. Introduction

With the progressive reduction of emissions from large combustion plants, from road traffic, the emissions from other sources, as non-road mobile sources, are becoming increasingly important, in particular in port areas where intense commercial activities are present. Many cities in Europe and even in Italy have great difficulties in compliance with the limits imposed by European Union legislation on air quality. The presence of harbors/ports in urban areas should be considered as an important pollution source, often also with the presence of cruise terminals, which are completely integrated into the cities. Furthermore, the International Maritime Organization (IMO) has estimated

that more than 90% of world trade is moved by sea as the maritime transport is the cheapest way to move goods and raw materials [1].

In large harbors, air quality is measured by monitoring the atmospheric concentrations of the pollutants regulated by Legislative Decree 155/10 [2], such as nitrogen dioxide (NO₂), sulfur dioxide (SO₂), carbon monoxide (CO), ozone (O₃), benzene (C₆H₆), PM₁₀ and PM_{2.5} through mobile and fixed monitoring stations.

Among the most polluting factors, besides land-based port activities, the main ship emissions are nitrogen oxides (NO_x), sulfur oxides (SO_x), CO, particulate matter (PM) and hydrocarbon (HC) due to the engine combustion [3–6]. Ship emissions account for respectively 2.7%, 15% and 4–9% of the global anthropogenic CO₂, NO_x and SO₂ emissions [7], whereas PM₁₀ and PM_{2.5} levels are related to primary emissions from fuel oil combustion but also to the formation of secondary aerosols [8]. These pollutants are the main chemicals involved in processes leading to acidification and eutrophication as well as formation of ground level ozone [9]. The pollution of port cities is mainly due to the stationing of cruise ships moored to the piers [10]—these floating cities must keep the engines running both to work and to provide on-board passenger services [11]. By this way, highly toxic fumes are emitted into the atmosphere compromising the air quality [12], the environment [13] and, consequently, the public health [14,15]. Based on previous evidences [16–18], it can be hypothesized a specific role of environmental pollution of industrial origin on the current frequency of lung cancer in Civitavecchia. Infant respiratory disease is strongly influenced by environmental exposures. Recent studies conducted in Europe and the United States have highlighted a role of air pollution in the aggravation of bronchial asthma, a pathology particularly frequent in pediatric age [19–21]. As a consequence, in complex areas where multiple sources are located, the study of contribution to PM emission from different sources is an important task in air quality management. These studies are performed using the source apportionment methodologies [22–25]. The possibility to discriminate among different emission sources and between natural and anthropogenic contribution is a key issue for planning efficient air pollution reduction and mitigation strategies, as pointed out by different authors [26–28]. Moreover, the knowledge of the chemical composition [29,30] for the different PM size is recognized as increasingly important, in particular with respect to the health effects of the exposed population [31]. All the considerations will be based on data obtained from wind-oriented samplings. This particular strategy, still considered rare, was introduced by Alleman et al. [32]. Each sampler, coupled with a wind sensor allowing the turning on and off of the instrument depending on wind direction and speed, alternately collects PM coming from the wind directions—in this way, each airborne sample, related to different wind conditions, is not predominantly associated with a direction but is exclusively connected with a single direction [33–35]. Figure 1 shows the sampler used in this study.



Figure 1. Wind-selective samplers used in this campaign.

The aim of this study is the identification of main emitting sources of PM₁₀ and PM_{2.5} in the Civitavecchia port-industrial area (Central Italy), namely a large coal-fired power plant, a natural gas power plant, the harbor activities, the vehicular traffic (due to urban traffic and to the highway crossing the area) and small industrial companies located in the town. Our study also provides precious information on the chemical composition of the PM₁₀ and PM_{2.5} collected, effective to explain specific sources emission patterns as well as to assess the concentration levels of micro pollutants (MPs), particularly toxic for human health.

2. Experiments

Characterization of the Sampling Site

The investigated area (Figure 2) is affected by the presence of different anthropogenic sources. Civitavecchia is a city of about 53,000 inhabitants, hosting a commercial port which moves about 4 million people and 11 million tons of goods per year. In recent years, it has become a leading port for cruise ships in the Mediterranean Sea. Furthermore, Civitavecchia is the third Italian energy hub, with a coal-fired power plant (Torrevaldaliga North) of 1980 MW and gas turbine plant (Torrevaldaliga South) of a 1200 MW. This area is crossed by an important highway (Rome-Tarquinia) and the Aurelia state road is affected by freight traffic.

With the aim to study the sources contribution to PM environmental concentrations, the chosen sampling method is represented by a PM sampler coupled with a wind-select sensor that allows collecting PM on different cartridges according to specific wind directions (WindSelect+, MonitoringSystems GmbH, Austria). In fact, this device allows to set two user-defined wind direction sectors, corresponding to specific emission sources (i.e., coal-fired power plant, sector #1 and harbor, sector #2). By this way, the wind sensor activates the different cartridge and acquires the air volumes when the wind comes from these wind sectors; a third sector (sector #3) is activated when the wind blows from all other directions.

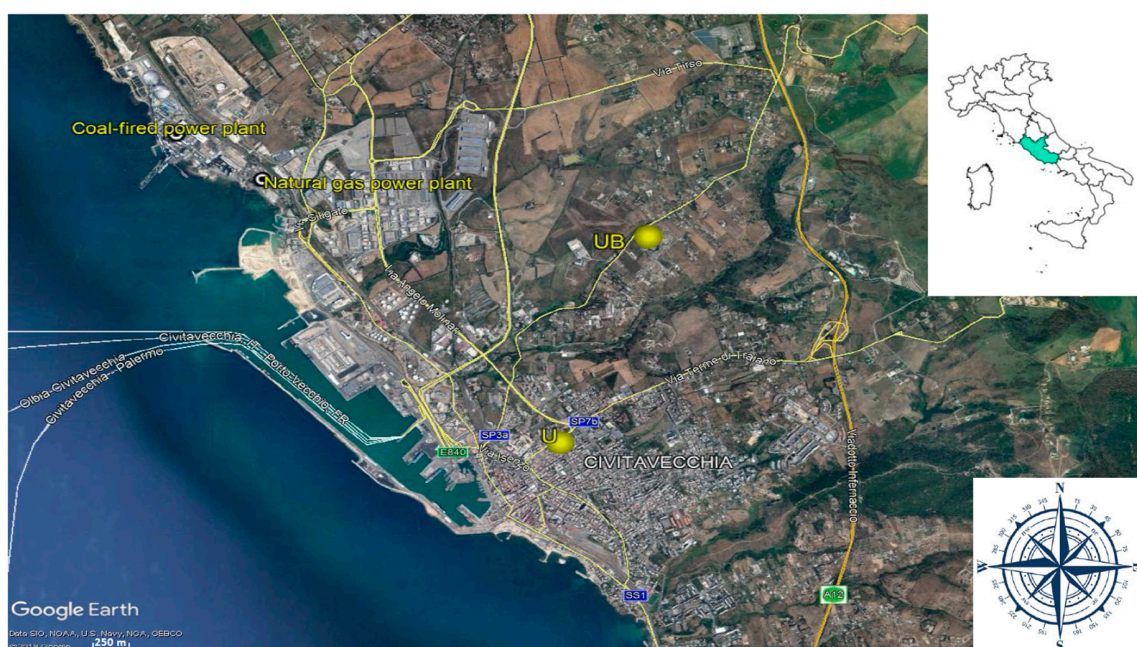


Figure 2. Map of the harbor-industrial area in Civitavecchia—the coal-fired power plant, the natural gas power plant and the two sampling sites, that is, U located in downtown Civitavecchia and Urban Background (UB) located outside the urban area, are identified.

In this study, two sampling sites have been identified in the area—the first inside the densely populated urban area of Civitavecchia, downtown Civitavecchia (U), was placed on the roof of a public

building at about 25 m above the ground level, the second one was located just outside the urban area, in an Urban Background (UB) site, at 3 m above the ground level. The U and UB sites, both equipped with a PM₁₀ and PM_{2.5} wind-select sampling device, are 12 km apart. The samplers have been configured to collect airflows downwind the coal-fired power plant (sector #1) and downwind the port area (sector #2), whereas all other wind directions correspond to sector #3. For the U site the sectors were—sector #1: 300°–330°, downwind the coal-fired power plant direction; sector #2: 200°–280°, downwind harbor; sector #3: all other directions. For the UB site the three sectors were: sector #1: 270°–300°, downwind coal-fired power plant direction; sector #2: 210°–260°, downwind harbor; sector #3: all other directions.

The study was carried out from July 2015 to June 2016. PM₁₀ and PM_{2.5} samplings were performed by means of wind-selective samplers; the duration of each sampling was approximately 30 days. On the PM₁₀ and PM_{2.5} samples monthly collected, chemical analyses were performed for determining the concentrations of organic and inorganic species in both aerosol size filters, focusing on those related to coal combustion, as heavy metals (i.e., As, Cd, Mn, Ni, Pb, Se, V, etc.), Polycyclic Aromatic Hydrocarbons (PAHs), Polychlorinated Biphenyl (PCBs), Polychlorodibenzodioxins and Polychlorodibenzofurans (PCDD/Fs) [36–41]. For the depositions, the measurements were carried out with bulk samplers according to UNI EN 15841:2010 and UNI EN 15980:2011 standards. The detection system consists of glass fiber filters and adsorbent cartridges (Polyurethane Foam, PUF, and Amberlite XAD-2). For the organic compounds the samples were extracted by Accelerated Solvent Extraction (ASE) and the analyses were carried out by HRGC-HRMS (High Resolution Mass Spectrometry; R > 10,000), according to the indications of UNI EN 1948:2006 parts 2 and 3, for the determination of PCDD/Fs and PCBs and according to the indications of ISO 122,844 and UNI EN 15549:2008 (specifically for benzo (a)pyrene) for determining PAHs whereas the determination of the inorganic fraction, that is, metals, was performed by IPC-MS, according to UNI EN 14907:2005, after that the samples were mineralized in HNO₃ according to the UNI EN 14902:2005. Finally, a particular attention was devoted to investigating the Limit of Detections (LODs) of each compound; they can be resumed as follows—metals 0.1 ng; PAHs 10 ng; PCDD/Fs 100 fg; PCB 1000 fg.

3. Results and Discussion

An analysis on the meteorological conditions of the area and on operating characteristics of the coal-fired power plant was initially performed.

3.1. Meteorological Conditions

The analysis of the meteorological conditions was carried out on data acquired from the meteo-station located inside the coal-fired power plant settlement at high altitude (120 m).

The available data cover the period between June 2015 to March 2016. The analysis of wind directions showed the expected seasonal variability during all the study period. In general, the winds from East have low frequencies, in some periods they are absent. The most frequent directions are those associated with the sector from South-West to North-West, the winds from the South are predominant in the months of October and February, whereas the North-East sector is present with higher frequencies in the months of September, October, November and March.

Figure 3 shows how the wind directions change during the daily hours, as measured in the period June 2015–March 2016. Until mid-morning hours the North-East and South-East directions are prevalent, therefore the wind turns and during the afternoon West and North-West sectors are the predominant wind directions, in particular the North North-West sector during the evening (hours 16–19). Even the wind speeds show a variability strictly related to wind direction. On average, higher speeds are associated with winds from the North-East and South-East directions. A frequency analysis of the daily hours in which the wind sectors are active was also performed. Sector #1 of the U site is downwind more frequently during the evening hours, the other sectors, that is, sector # 2 of U site and sectors # 1 and # 2 of UB site, are downwind more frequently during the mid-day hours and early afternoon.

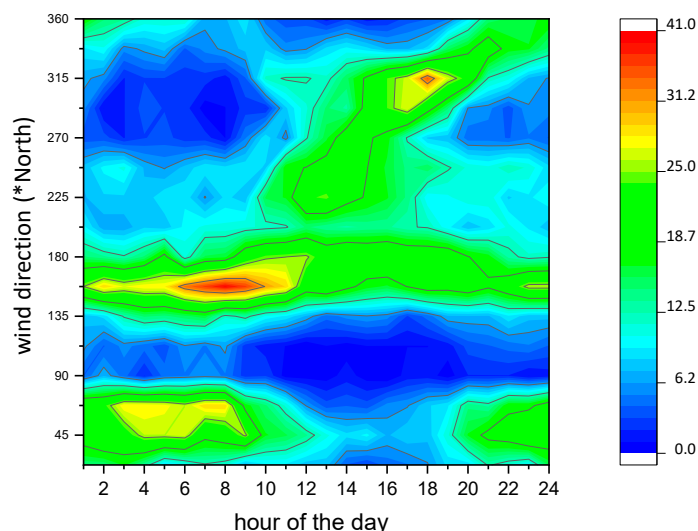


Figure 3. Frequency distribution of wind directions according to the daily hours.

3.2. Coal-Fired Power Plant Information

The analysis of operation characteristics of the coal power plant was performed, taking into account data from the Continuous Monitoring System installed on the three stacks (Table 1). Total Suspended Matter (TSM) emission data (in mg Nm^{-3}) from the period June 2015 to March 2016 were analyzed.

Table 1. Main Plant Operation during the Entire Sampling Campaign (June 2015–March 2016).

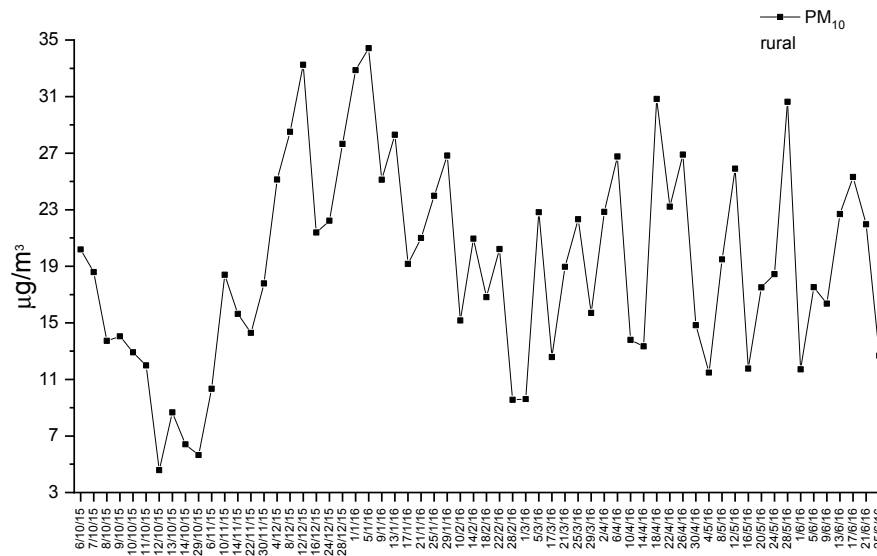
Time	Group 2			Group 3			Group 4		
	Capacity ^a	Flow Rate ^b	TSM ^c	Capacity ^a	Flow Rate ^b	TSM ^c	Capacity ^a	Flow Rate ^b	TSM ^c
June	550(43)	1,572,272	2.2	596(79)	2,075,928	1.8	601(99)	1,909,308	1.5
July	591(100)	1,664,146	1.9	575(95)	2,019,210	1.8	528(100)	1,745,957	1.7
August	576(99)	1,615,357	2.6	527(100)	1,905,924	2.1	438(100)	1,527,666	1.9
September	594(90)	1,757,349	2.3	577(99)	2,066,819	1.4	521(87)	1,768,322	1.8
October	551(51)	1,665,602	2.2	573(61)	2,048,259	1.2	547(100)	1,891,623	1.5
November	605(98)	1,839,608	2.2	582(80)	2,047,368	1.2	562(99)	1,929,248	1.8
December	616(95)	1,958,688	2.1	582(65)	1,487,230	1.3	595(100)	2,023,051	1.8
January	590(100)	1,981,041	2.2	504(93)	2,049,992	1.6	581(90)	1,969,306	1.7
February	500(97)	1,645,718	2.8	547(100)	1,859,879	1.6	533(64)	1,812,716	2.5
Mar	535(88)	1,772,537	2.7	543(99)	1,825,371	1.7	445(29)	1,478,600	4.4

^a expressed as MW (% of operation); ^b expressed as $\text{Normal m}^3 \text{ h}^{-1}$; ^c expressed as mg Nm^{-3} .

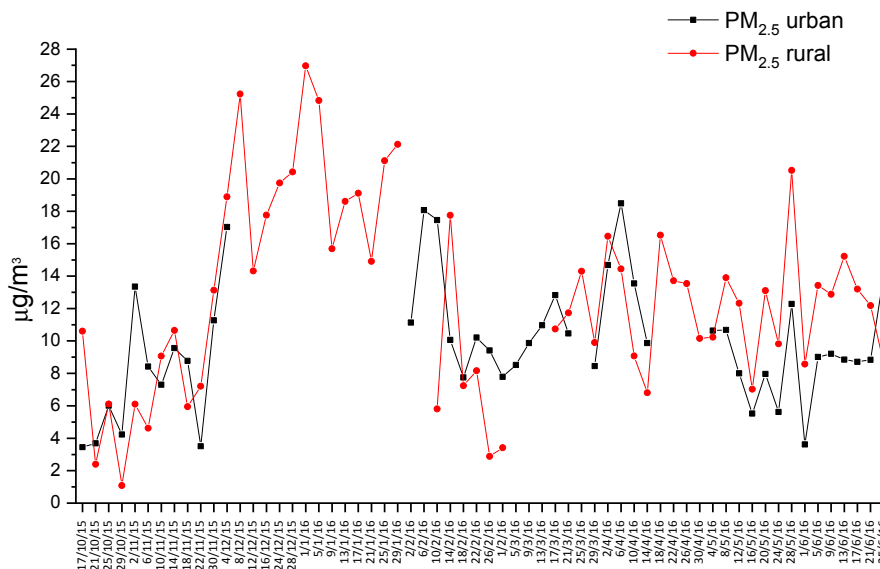
3.3. Chemical Analysis and Relative Source Apportionment

As said before, the study was addressed for identifying the sources (source apportionment) of organic and inorganic contaminants in similar complex areas, using the wind-select monitoring devices. This approach allows to highlight the relationships between the presence/abundances of specific chemicals and the wind/sampling directions. Further, before starting with the results, it should be underlined that the domestic heating, another well-known source potentially affecting the urban air quality, in Civitavecchia is characterized by methane gas—in this case the authors considered its contribution to be superfluous, also considering the average temperatures ranging between 13.5–21.1 °C during winter/autumn period and 17.3–25.9 °C during spring/summer period, with a yearly average of 19.5 °C, 66 rainy days and Relative Humidity (RH) 74.7% (source—Stazione Meteorologica di Civitavecchia).

At the same time, concentrations data of PM_{10} at the suburban site and $\text{PM}_{2.5}$ in the two sites, urban and suburban locations, were acquired for all the period. These data were measured by gravimetric method with instrument located close to the wind-select samplers. Figure 4 shows the gravimetric measurements performed in urban and suburban area—particularly, Figure 4a shows the PM_{10} behavior for the entire period whereas Figure 4b $\text{PM}_{2.5}$ in both locations.



(a)



(b)

Figure 4. Gravimetric measurements in the two sites—PM₁₀ in suburban area (a) and PM_{2.5} in the two sites (b).

In the urban area, due to maintenance works, data of PM_{2.5} are missing between December and January, (in Figure 4b there is a “hole” in that period). The concentrations are similar on both sites—at the suburban site, an average value of 12.6 $\mu\text{g m}^{-3}$ is recorded whereas at urban site a mean value of 9.7 $\mu\text{g m}^{-3}$. This is most likely due to the missing measurement period (December–January) at this location—in fact, wintertime shows unfavorable meteorological conditions for the pollution dispersion [42,43], allowing high levels of pollutants. PM₁₀ measurements at the suburban site show a mean value of 19 $\mu\text{g m}^{-3}$ for the entire period—the measurements confirm the high pollution level recorded during January and December period as provided by the Figure 4a.

The results of chemical analysis performed on PM_{2.5} and PM₁₀ are represented in Tables 2 and 3 for the mean levels of inorganic (i.e., metals) and organic (PCDD/Fs, PAHs and PCB and DL-PCB) substances in cartridges sampled for each sector. Data in Tables 2 and 3 concern the whole period mean concentration of each pollutants both in urban and suburban site. In Tables S1–S8 of the Supplementary Material report all the analytical determinations performed sector-by-sector during the whole sampling periods in both locations are reported.

Table 2. Levels of Metals, Polycyclic Aromatic Hydrocarbons (PAHs), Polychlorinated dibenzodioxins and Polychlorinated dibenzofurans (PCDD/Fs) and Polychlorinated biphenyls (PCBs) determined in downtown (site U).

Compound	PM ₁₀			PM _{2.5}		
	Sector #1	Sector #2	Sector #3	Sector #1	Sector #2	Sector #3
<i>Metals (ng m⁻³)</i>						
As	1.73	0.310	0.076	1.27	0.210	0.114
Ba	6735	1852	293	38.7	3.13	0.628
Be	0.144	0.035	0.006	0.040	0.006	0.001
Cd	3.12	0.763	0.076	0.615	0.051	0.034
Co	0.549	0.066	0.022	0.666	0.172	0.030
Cr	79.3	10.2	1.64	218	31.9	3.46
Cu	22.1	3.11	1.70	21.8	3.36	1.39
Mn	20.2	1.65	0.725	27.7	1.53	0.445
Ni	22.0	2.40	0.764	32.7	6.36	1.94
Pb	35.3	5.77	0.724	8.19	2.31	1.34
Sb	5.75	0.311	0.091	2.95	2.94	0.437
Se	2.42	0.311	0.055	0.588	0.206	0.155
Sn	8.81	0.856	0.438	8.90	1.58	0.594
Sr	17.3	5.54	1.46	18.1	0.83	0.302
Te	0.031	0.001	0.001	0.017	0.013	0.000
Ti	16.9	2.18	0.6223	26.06	1.455	0.360
Tl	0.299	0.006	0.003	0.030	0.115	0.004
V	15.1	0.918	0.154	6.76	5.46	1.56
Zn	8138	2770	387	70.9	15.6	6.64
<i>Total Metals (ng m⁻³)</i>	<i>15,124</i>	<i>4656</i>	<i>688</i>	<i>484</i>	<i>77.2</i>	<i>19.4</i>
<i>PAHs (ng m⁻³)</i>						
Acenaphthene	4.97	0.631	0.043	26.5	3.42	2.14
Acenaphthylene	2.24	0.563	0.024	8.78	1.74	0.115
Anthracene	9.01	9.94	0.309	6.86	8.65	8.97
Benz[a]Anthracene	1.37	0.571	0.070	0.988	2.18	0.255
Benzo(a)pyrene	1.13	0.031	0.006	0.153	0.108	0.078
Benzo[b]Fluoranthene	1.22	0.031	0.049	0.153	0.031	0.151
Benzo[g,h,i]Perylene	1.50	0.031	0.066	0.274	1.08	0.127
Benzo[j]Fluoranthene	0.329	0.031	0.006	0.153	0.031	0.166
Benzo[k]Fluoranthene	0.424	0.031	0.004	0.153	0.031	0.311
Chrysene	1.62	0.464	0.077	0.863	1.31	0.253
Dibenzo[a,e]Pyrene	0.153	0.031	0.004	0.249	0.031	0.004
Dibenzo[a,h]Anthracene	5.11	0.031	0.004	0.280	0.031	0.065
Dibenzo[a,h]Pyrene	0.153	0.031	0.004	0.153	0.031	0.004
Dibenzo[a,i]Pyrene	0.153	0.031	0.004	0.153	0.031	0.004
Dibenzo[a,l]Pyrene	0.153	0.041	0.004	0.153	0.031	0.004
Phenanthrene	22.0	22.3	0.165	91.2	3.85	4.76
Fluoranthene	1.48	0.040	0.325	29.7	5.48	1.1198
Fluorene	11.7	1.95	0.245	54.0	9.95	1.40
Indeno [1,2,3-cd]Pyrene	1.50	0.031	0.051	0.291	0.964	0.123
Naphthalene	374	44.4	0.723	2189	373	45.6
Pyrene	3.43	1.07	0.087	19.0	9.22	2.30
<i>Total PAHs</i>	<i>64.7</i>	<i>36.8</i>	<i>1.41</i>	<i>221</i>	<i>38.0</i>	<i>19.9</i>
<i>PCDD/Fs (fg m⁻³)</i>						
2,3,7,8-TCDD	1.53	0.314	0.038	1.53	0.314	0.233

Table 2. Cont.

Compound	PM ₁₀			PM _{2.5}		
	Sector #1	Sector #2	Sector #3	Sector #1	Sector #2	Sector #3
1,2,3,7,8-PCDD	3.99	1.51	0.038	1.53	0.604	1.25
1,2,3,4,7,8-HxCDD	1.53	0.314	0.100	1.53	0.314	0.336
1,2,3,6,7,8-HxCDD	13.6	0.314	0.250	1.53	0.611	0.729
1,2,3,7,8,9-HxCDD	12.6	0.314	0.143	1.53	0.544	0.793
1,2,3,4,6,7,8-HpCDD	92.7	0.886	1.14	38.1	9.47	11.4
OCDD	601	29.0	3.64	878	694	53.7
2,3,7,8-TCDF	27.4	1.93	0.149	24.15	5.84	8.90
1,2,3,7,8-PCDF	1.53	0.314	0.344	3.11	1.86	1.39
2,3,4,7,8-PCDF	32.4	0.558	0.345	1.53	6.14	4.58
1,2,3,4,7,8-HxCDF	27.0	0.487	0.633	3.59	2.94	4.42
1,2,3,6,7,8-HxCDF	30.7	0.314	0.636	5.30	1.16	2.76
2,3,4,6,7,8-HxCDF	16.9	1.534	0.852	4.47	1.84	6.58
1,2,3,7,8,9-HxCDF	4.63	0.314	0.221	1.53	0.397	0.244
1,2,3,4,6,7,8-HpCDF	79.2	4.08	2.39	26.3	6.66	15.1
1,2,3,4,7,8,9-HpCDF	10.7	0.919	0.229	1.53	1.03	1.35
OCDF	264	5.13	3.32	107	18.7	12.5
Total PCDD/Fs	1221	48.2	14.5	1102	752	126
<i>PCBs (fg m⁻³)</i>						
77-CB	84.5	11.2	1.09	3945	439	179
81-CB	15.3	3.94	0.920	148	49.2	20.3
105-CB	804	58.7	27.3	4580	2099	873
114-CB	28.6	7.44	0.700	323	202	112
118-CB	10,402	1175	303	40,712	7404	2843
123-CB	128	33.2	10.8	4041	208	201
126-CB	15.3	9.36	0.807	29.5	12.4	4.31
156-CB	2694	382	68.5	10174	886	153
157-CB	76.4	20.6	1.88	122	25.7	5.07
167-CB	1043	93.5	33.9	896	532	44.7
169-CB	15.3	9.09	0.377	15.3	3.14	4.67
189-CB	535	25.1	6.26	277	79.8	23.6
Total PCBs	15,841	1829	456	65,263	11,940	4464

Table 3. Levels of Metals, PAHs, PCDD/Fs and PCBs determined at suburban area (Site UB).

Compound	PM ₁₀			PM _{2.5}		
	Sector #1	Sector #2	Sector #3	Sector #1	Sector #2	Sector #3
<i>Metals (ng m⁻³)</i>						
As	0.614	2.35	0.074	0.190	0.218	0.070
Ba	2379	6425	132	2.61	7.04	0.713
Be	0.046	0.137	0.004	0.003	0.012	0.001
Cd	0.146	0.317	0.013	0.035	0.057	0.034
Co	0.067	0.216	0.017	0.092	0.172	0.022
Cr	3.18	12.4	0.351	26.0	98.7	2.25
Cu	1.92	8.24	0.594	2.90	3.37	1.16
Mn	0.797	2.38	0.493	1.91	5.40	0.175
Ni	3.22	4.97	0.294	3.33	6.75	0.734
Pb	1.56	4.68	0.243	1.31	1.93	1.22
Sb	0.122	2.95	0.047	0.270	0.667	0.96
Se	0.253	1.02	0.047	0.145	0.143	0.086
Sn	1.80	16.1	0.409	3.04	4.73	1.27
Sr	2.88	24.8	1.19	1.47	3.09	0.100
Te	0.010	0.007	0.001	0.003	0.007	0.000
Ti	0.763	3.40	0.340	1.01	3.09	0.215
Tl	0.020	0.017	0.000	0.010	0.010	0.013
V	0.327	0.843	0.096	1.95	1.34	0.792
Zn	2873	9581	283	8.96	19.3	2.90

Table 3. Cont.

Compound	PM ₁₀			PM _{2.5}		
	Sector #1	Sector #2	Sector #3	Sector #1	Sector #2	Sector #3
<i>Total Metals</i>	5270	16,091	420	55.2	156	12.7
<i>PAHs (ng m⁻³)</i>						
Acenaphthene	0.598	2.04	0.017	1.23	7.27	1.23
Acenaphthylene	0.063	0.918	0.006	0.333	5.34	0.056
Anthracene	1.23	2.46	0.061	1.15	6.82	0.301
Benz[a]Anthracene	0.242	720	0.004	1.76	0.958	0.115
Benzo(a)pyrene	0.017	0.142	0.003	0.132	1.51	0.031
Benzo[b]Fluoranthene	0.017	16.1	0.005	0.412	0.728	0.152
Benzo[g,h,i]Perylene	0.017	0.107	0.003	0.512	1.08	0.104
Benzo[j]Fluoranthene	0.017	0.124	0.002	0.038	0.182	0.089
Benzo[k]Fluoranthene	0.017	0.068	0.004	0.025	0.189	0.065
Chrysene	0.188	0.124	0.005	1.19	3.38	0.327
Dibenzo[a,e]Pyrene	0.017	0.068	0.002	0.017	0.094	0.044
Dibenzo[a,h]Anthracene	0.017	0.068	0.002	0.017	0.068	0.029
Dibenzo[a,h]Pyrene	0.017	0.068	0.002	0.017	0.068	0.002
Dibenzo[a,i]Pyrene	0.017	0.068	0.002	0.017	0.068	0.002
Dibenzo[a,l]Pyrene	0.017	0.068	0.002	0.017	0.068	0.047
Phenanthrene	0.727	0.958	0.038	12.3	22.6	10.4
Fluoranthene	1.02	2.22	0.057	5.83	13.9	5.05
Fluorene	1.15	8.70	0.073	1.94	9.35	2.86
Indeno[1,2,3-cd]Pyrene	0.017	0.104	0.004	0.340	0.739	0.066
Naphthalene	1.43	4.81	0.119	188	910	23.4
Pyrene	0.783	1.78	0.043	3.15	7.24	3.54
<i>Total PAHs</i>	5.39	754	0.288	27.0	73.7	20.9
<i>PCCD/Fs (fg m⁻³)</i>						
2,3,7,8-TCDD	0.167	2.56	0.022	0.304	0.925	0.114
1,2,3,7,8-PCDD	1.07	5.34	0.067	0.167	80.7	1.38
1,2,3,4,7,8-HxCDD	0.381	6.07	0.037	0.656	0.685	1.23
1,2,3,6,7,8-HxCDD	0.435	12.2	0.081	0.975	1.47	4.65
1,2,3,7,8,9-HxCDD	0.395	11.1	0.095	0.353	0.685	4.56
1,2,3,4,6,7,8-HpCDD	2.45	94.7	1.70	6.85	15.2	38.8
OCDD	14.3	261	4.16	19.8	106	79.4
2,3,7,8-TCDF	2.01	18.3	1.23	5.95	7.29	8.85
1,2,3,7,8-PCDF	0.851	8.74	0.071	0.937	2.45	4.94
2,3,4,7,8-PCDF	1.34	26.4	0.479	2.43	10.1	10.6
1,2,3,4,7,8-HxCDF	1.07	37.6	0.330	2.40	5.69	14.6
1,2,3,6,7,8-HxCDF	0.696	30.3	0.321	1.51	4.66	10.9
2,3,4,6,7,8-HxCDF	0.943	54.8	0.783	1.84	3.50	17.9
1,2,3,7,8,9-HxCDF	0.505	7.30	0.056	0.296	1.18	4.38
1,2,3,4,6,7,8-HpCDF	4.32	237	2.22	11.6	14.8	79.0
1,2,3,4,7,8,9-HpCDF	1.19	9.13	0.103	0.610	2.11	9.51
OCDF	8.12	175	3.13	9.91	17.2	101
<i>Total PCCD/Fs</i>	40.3	997	14.9	66.6	275	392
<i>PCBs (fg m⁻³)</i>						
77-CB	19.2	28.8	0.580	1033	3752	166
81-CB	3.92	6.85	0.217	92.9	85.3	7.29
105-CB	101	555	26.0	1729	6340	249
114-CB	1.46	7.58	0.535	92.3	580	11.8
118-CB	1421	4444	191	7023	26,709	1192
123-CB	12.5	28.8	1.10	164	1826	22.0
126-CB	1.67	6.85	0.217	14.9	6.85	2.01
156-CB	666	1750	68.3	453	2606	104
157-CB	19.8	34.2	2.10	8.36	34.2	1.10
167-CB	276	630	22.7	287	1103	62.4
169-CB	1.67	6.85	0.217	1.67	6.85	1.48
189-CB	53.4	184	2.21	13.7	84.9	7.04
<i>Total PCBs</i>	2578	7683	315	10,912	43,134	1826

3.3.1. Inorganic Fraction

The study of inorganic substances has been addressed for elements potentially representative of anthropic sources with high interest for public health. With this aim, in addition to the metals routinely monitored in compliance with the air quality law (Legislative Decree 155/2010), that is, As, Cd, Ni and Pb, the chemical analysis also concerned Sb, Ba, Be, Co, Cr, Mn, Cu, Se, Sr, Tl, Te, Ti, V and Zn. These elements are generally present with different abundances and in different oxidation states in the PM size fractions.

The analytical determinations of metals for each monitoring site and both PM fractions and sectors, are showed in Tables S1 and S2 of the Supplemental Material for the U and UB sites, respectively. Figure 5a,c for U site and Figure 5b,d for UB site, respectively, report all the concentrations measured during the entire sampling period.

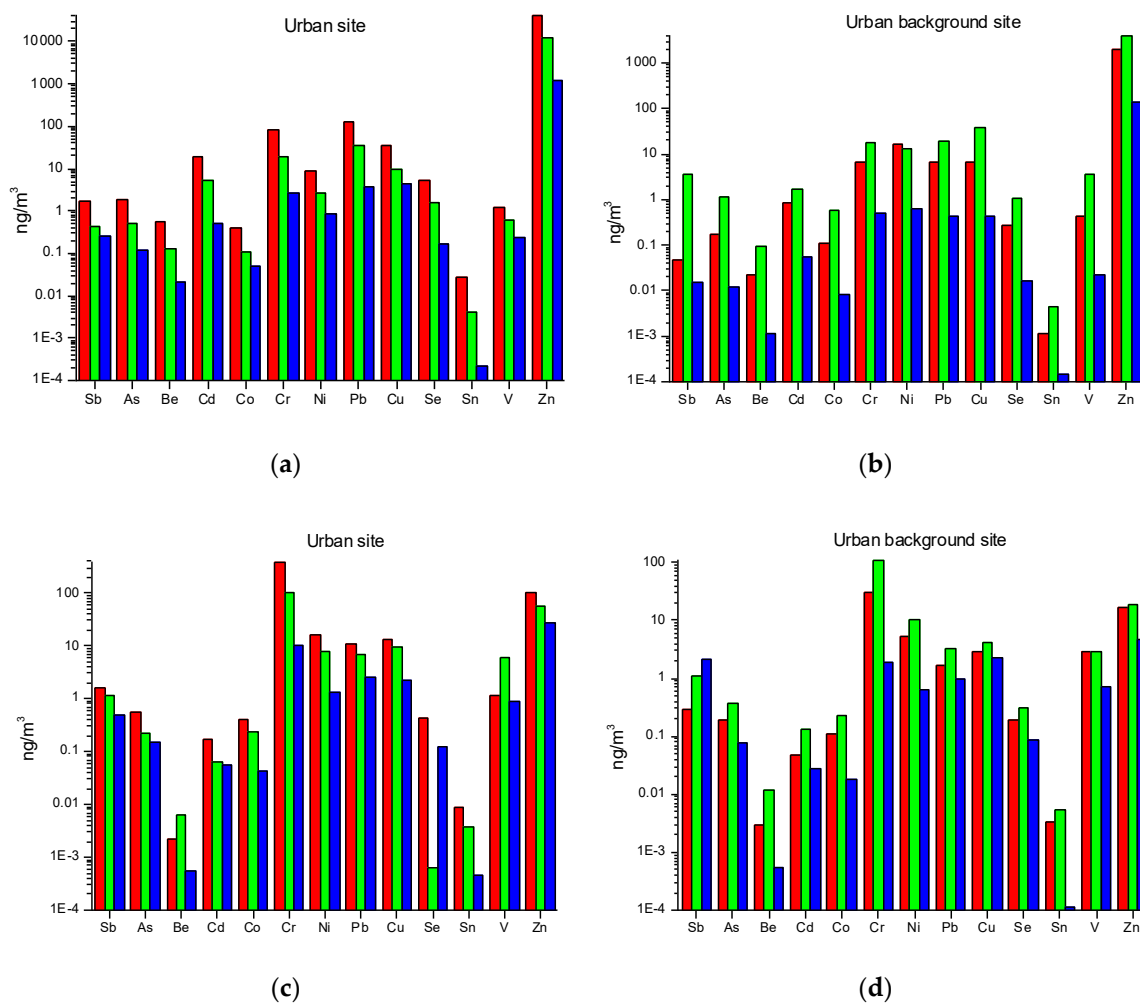


Figure 5. Metals and metalloids in PM_{10} and $\text{PM}_{2.5}$ in the (a,c) Urban Site and (b,d) Urban Background, respectively—both the PM fractions highlight the presence of many anthropogenic elements; it is also worth noting the predominance of Cr_{tot} in the $\text{PM}_{2.5}$ fraction in both sampling sites, which can be associated to coal combustion (red: sector #1; green: sector #2; blue: sector #3).

For a comparison of concentration values measured regulated metals (As, Cd, Ni and Pb) with limit established by regulation, it must be taken into account the different sampling methods used with those defined by law. For the regulated metals, it is possible a comparison only for determinations on the PM_{10} fraction, even though the integration time of PM_{10} in this study is on monthly average and not daily as required.

Taking into account this caution, the following values deserve to be mentioned:

- ✓ For the U site, sector #1, Cd 18.6 ng m⁻³ in autumn, As 6.67 ng m⁻³ and Ni 62.3 ng m⁻³ in spring period and 58.7 ng m⁻³ in summertime;
- ✓ For the UB site, sector #2, As 9.86 ng m⁻³ in autumn and Ni 35.0 ng m⁻³ in summertime.

For other metals, in both stations, there is a higher percentage presence of Ba, Cr and Zn compared to the other metals. Further, in both stations, Cr shows peak concentrations mainly in the PM_{2.5} fraction, whereas Ba and Zn have the highest concentrations in the PM₁₀ fraction. The different distribution of heavy metals in the two fractions, sometimes higher concentrations in the *fine* fraction than in PM₁₀, is strange but not surprisingly. Such occurrence was found in other studies, also by some co-authors in samples collected downtown [44] or in industrial area [45].

The wind-selective analysis aims to highlight the pollutant origin, as the study main objective. On this regard, the inorganic fraction in PM₁₀ and PM_{2.5} shows the following:

- For U station the highest metal concentration values are recorded in sector #1, downwind the coal-fired power plant, both in the PM₁₀ and in the PM_{2.5} fraction;
- For the UB station the highest levels are, on average, recorded at sector #2, downwind the port area, both in the PM₁₀ fraction and in the PM_{2.5} fraction.

Except for As, Ba, Se, Te and Zn, the higher concentration values for each element are observed at the U station. Some exceptions for specific chemicals are noted, mainly in the sector #2—Cr and Co in the PM_{2.5} fraction in winter and Ba, Sr and Zn in the PM₁₀ fraction in summer. For the UB location, Zn in the PM₁₀ fraction in the summer period when sector #3 is prevailing, Cu in the PM_{2.5} fraction in the autumn period during sector #1 prevailing and Ni in the PM₁₀ fraction in the autumn period with high frequency of sector #1.

3.3.2. Organic Fraction

For organic pollutants, the concentration profiles of PAHs, PCCD/Fs and PCBs in the PM₁₀ and PM_{2.5} fractions were studied.

In general the urban location measures higher PAH concentrations than the suburban one, even though the concentrations always remain below values compatible with the monitored urban territorial context, and, the benzo (a)pyrene (B (a)P) concentrations, that is, the only PAH regulated by Legislative Decree 155/2010 [1], in PM₁₀ are always lower than 1.0 ng m⁻³ which is the limit for the annual average. Just one measure (Tables S3 and S4 of the Supplementary Material), performed in U site records a concentration of B(a)P greater than 1.0 ng m⁻³.

Comparing the PAHs concentrations measured in the different sectors (Figure 6), sector #1 of the U location averagely records higher values than those observed in sectors #2 and #3, whereas in the UB area sector #2 records higher concentrations than those in sectors #1 and #3. Sectors #3 of both stations record the lowest PAHs concentrations.

Comparing the measures performed, it is noted that each PAH is concentrated in the PM_{2.5} fraction in all samplings carried out during the entire research study, except for measures performed at U area sector #1 during springtime, when some PAHs are below the LODs in PM_{2.5} fraction whereas they are observed in PM₁₀ samples. For the UB location the measures always show higher concentrations in PM_{2.5}; only once they are higher in PM₁₀ for benzo(a)anthracene, B(a)P and benzo (b)fluoranthene, during the winter period.

The PAHs profile, representing the percentage of the concentration of each PAHs measured with respect the whole PAH concentration, can suggest some information on pollutants origin. Figure 7 shows the profiles of the mean PAHs levels for both the urban site during the winter period for each sector and particle size. Each profile is represented starting from the top to the bottom with the lightest PAH (2 benzene rings) to the heaviest (5–6 benzene rings). In U and UB site and in all sectors, naphthalene shows the highest concentration among the PAHs pollutants.

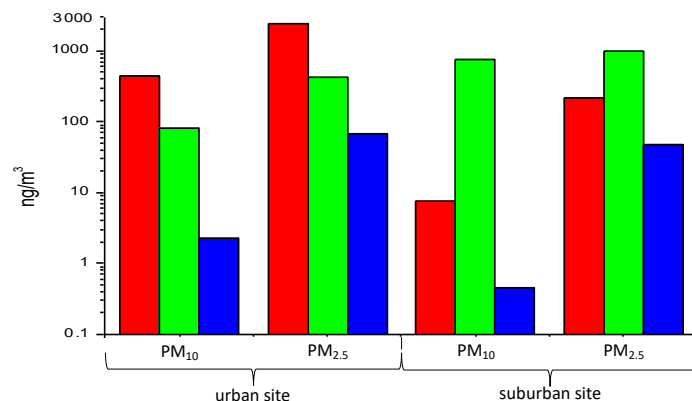


Figure 6. PAHs concentrations—sector #1 (air coming from the power plant) is the prevailing sector in U site, sector #2 (air coming from port area) in the UB site (red: sector #1; green: sector #2; blue: sector #3).

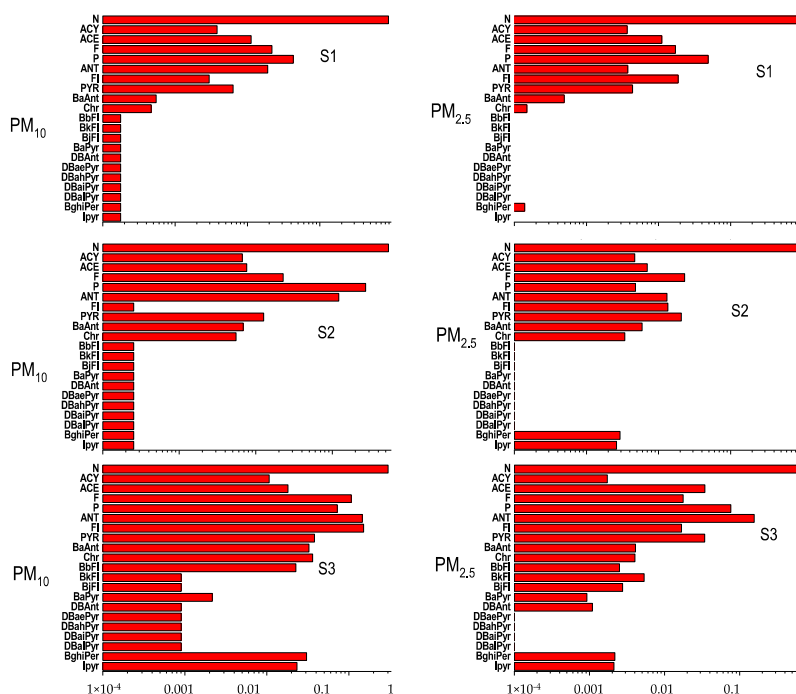


Figure 7. PAHs profiles for U site—naphthalene and phenanthrene, markers of ship emissions, show greater concentration in every sampling period and sector (in figure the spring sampling), indicating a significant contribution of port area to the overall emissions (N: Naphthalene; ACY: Acenaphthylene; ACE: Acenaphthene; F: Fluorene; P: Phenanthrene; ANT: Anthracene; Fl: Fluoranthene; Pyr: Pyrene; BaAnt: Benzo[a]anthracene; Chr: Chrysene; BbFl: Benzo[b]fluoranthene; BkFl: Benzo[k]fluoranthene, BjlFl: Benzo[j]fluoranthene; DBAnt: Dibenzoanthracene; DBa[e]Pyr: Dibenzo[a,e]pyrene; DBa[h]Pyr: Dibenzo[a,h]pyrene; DBa[i]Pyr: Dibenzo[a,i]pyrene; DBa[l]Pyr: Dibenzo[a,l]pyrene; BghiPer: Benzo[g,h,i]perylene; Ipyr: Indeno[1,2,3-cd]perylene).

In general, all the measurements show the greatest contribution of the light PAHs (2–3 rings), present not more than 2% in the various samples, compared to the heavier ones. Besides to naphthalene, PAHs are phenanthrene, fluoranthene, anthracene, acenaphthene, chrysene and pyrene are the more abundant pollutants. Among the heavier PAHs, benzo[g,h,i]perylene and indeno[1,2,3-cd]pyrene show concentrations above the LODs. Generally, these two pollutants are related to diesel vehicular emissions [46–52] whereas the petrol vehicle emissions are characterized by B[a]P and dibenzo[ah]anthracene emissions [53–57]. For coal combustion, the PAHs profiles are generally characterized by a high presence of fluoranthene, pyrene, phenanthrene and anthracene, to which the

chrysene and the isomer of benzo[k]fluorantene are added [58–61]. Regarding marine emissions, for ships at the port both in mooring and maneuvering, the PAHs fingerprint is represented by naphthalene, phenanthrene, pyrene, fluorene, followed by acenaphthylene and acenaphthalene [62–65].

The PAHs profiles observed in the two locations and for all the sectors show a predominant pyrogenic contribution, due to mixed contributions from the coal-fired power plant and from the port area. The high percentage of naphthalene, whose concentrations always remain comparable with those that normally occur in urban environments [66,67], would suggest a significant contribution from the emissions from the port area. Furthermore, the contribution of diffuse emissions arising from the port and the power plant, determines a PAH background contamination, especially for the lighter compounds (i.e., from naphthalene to chrysene). On this picture, under some circumstances, heavy vehicle diesel traffic adds its own contribution.

Like PAHs, the PCDD/Fs determinations (expressed as toxic equivalent, WHO-TE₂₀₀₅) in the two locations (Figure 8) show that sector #1 in U site records higher concentrations than those observed from the other two sectors, whereas for the UB location sector #2 records the highest concentrations compared to the other two.

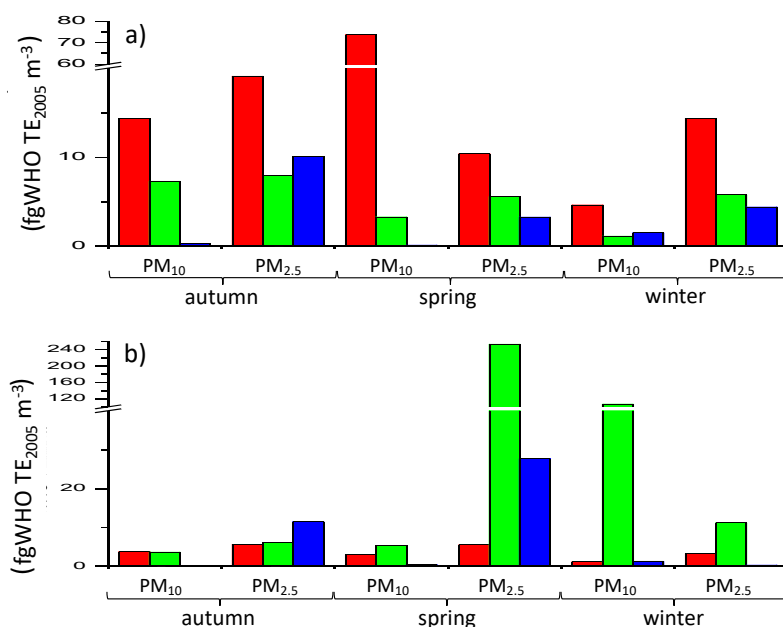


Figure 8. Polychlorinated dibenzodioxin and Polychlorinated dibenzofuran (PCDD/F) and Polychlorinated biphenyl (PCB) concentrations in (a) urban site and (b) suburban site—sector #3 shows during same monitoring period values greater or comparable with the other sectors suggesting a widespread contamination likely due to the presence of multiple emissive sources near the sampling site (red: sector #1; green: sector #2; blue: sector #3).

Differently from PAHs, the lowest concentrations of PCDD/F not always are related to sector #3. In U site the sector #3 concentrations are similar and, on two cases, higher than those recorded by sector #2. This behavior is also evident in the UB location, where the sector #3 concentrations, particularly in PM_{2.5} fraction, reach high concentrations compared to those measured in the other sectors. The Figure 8 shows that the UB station sector #2 records in the winter and spring high concentrations, an order of magnitude higher than all the others. Similarly, to the PAHs, the PCDD/F concentrations (in equivalent toxicity WHO-TE) are generally higher in PM_{2.5} with respect to PM₁₀, with the exceptions of spring-sector #1 U site and at spring-sector #2 of UB site. For the PCBs-DL (dioxin like) (Tables S7 and S8 of the Supplementary Material) comparable behaviors are highlighted in the two stations. In U site the higher concentrations are observed corresponding to sector #1, for the U site and to sector #2 for the UB area. In addition, pollutants concentrations are higher in the PM_{2.5} fraction compared to

PM₁₀. For PCBs-DL, the lowest concentrations are measured in relation to sector #3 for both stations, similarly to the PAHs behavior and differently from PCDD/Fs.

The Tables S5 and S6 of the Supplementary Material, respectively for U and UB sites, show the profiles of PCDD and PCDF congeners, for each sector, in PM₁₀ and PM_{2.5} fractions. A first analysis shows that the congener concentrations are not always higher in PM_{2.5} than PM₁₀. In fact, measures performed in autumn and spring for sector #1 in U site, show higher concentrations for some congeners in the PM₁₀ fraction as well as at UB area for the sector #1 in winter. Also, in spring the three sectors in the UB site show higher concentrations for almost all congeners in the PM₁₀ than in PM_{2.5}.

Furthermore, all measures performed during the study and the profiles of the DL-PCBs are reported in the Supplementary Material. The results show that the congeners 118-PCB; 105-PCB and 156-PCB give the highest contribution in all sectors, fractions and locations.

The PCDD/Fs profiles for the spring sampling period in UB site are represented in Figure 9. These are always predominated by the presence of OCDD and OCDF. The profiles of sector #1 for the PM_{2.5} fraction, show a similar behavior during the different samplings periods with predominance of OCDD and OCDF, whose summed contribution varies between 60% and 93%, while the secondary contributions are of TCDF, HxCDF and HpCDF.

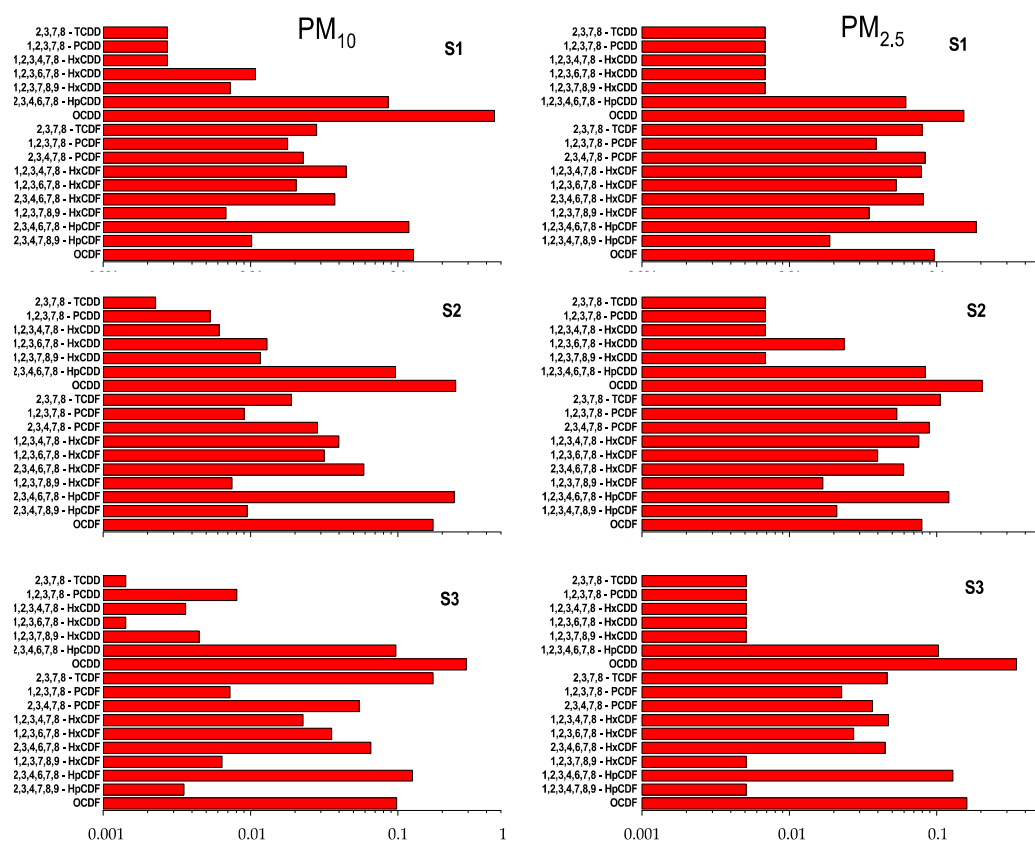


Figure 9. PCDD/F profiles in the UB site during spring sampling—the predominance of Octachlorodibenzodioxin (OCDD) and Octachlorodibenzofuran (OCDF) congeners is consistent with those reported by scientific literature in emissions from coal-fired power plant.

From the scientific literature [68–72] a similar profile is highlighted for PCDD/F emitted by large coal combustion plants. The PM₁₀ and PM_{2.5} profiles at U sector #1 are similar only in the autumn period, whereas they are different in the other two periods. The profiles of sector #2 of PM_{2.5} show greater variability, between periods and between congeners contributions. The PM₁₀ profiles at sector #2 differ from those of PM_{2.5} and show differences among periods in terms of detected congeners and their relative contribution. The PCDD/Fs profile sampled at sector #3 in PM_{2.5} shows a wide variability

of detected congeners in the different samples, according to the large sampling sector that cannot be associated with any specific source.

3.4. Chemometric Analysis

A statistical analysis has been carried out for overall the data. Preliminarily, a correlation among all the compounds has been investigated. In the U site the correlations between the PM fractions for the different sectors show a rather interesting trend. During autumn, high correlation coefficients (r) are observed between PM₁₀ and PM_{2.5} for sectors #1 and #3 (0.952, 0.950) whereas it is lower at sector #2 (0.662). For the other periods, the PM₁₀ and PM_{2.5} correlation coefficients are—in winter 0.878 sect #1, 0.975 sect #2, 0.882 sect #3; in summer 0.878 sect #1, 0.965 sect #2, 0.971 sect #3. The lower correlation coefficient in the autumn period between PM₁₀ and PM_{2.5} in sector #2 is probably due to a different weather condition, characterized by rapid changes of wind direction and speed, as expected in this season period. Different considerations can be drawn for the UB area—in the same period the correlation coefficient between PM₁₀ and PM_{2.5} is good, 0.847 and in the other periods r in the three sectors is better (>0.810 during autumn, >0.924 during winter, >0.912 during summertime). Very good correlation coefficients ($r > 0.970$) are observed comparing similar fractions in same sectors, for example, r between PM₁₀ in sector #1 urban area and PM₁₀ sector #1 in suburban area is 0.977. It should be underlined that the sectors were chosen in order to show the same sources in that direction (i.e., sector #1 downwind coal-fired power plant; sector #2 downwind the port area; sector #3 other directions).

Further, the authors approached to study the correlation coefficients (r) among the different inorganic and organic compounds investigated. Table 4 shows the r determined during the entire campaign.

Table 4. Correlation Coefficients (r) between PM₁₀ and PM_{2.5} Fractions among the Compounds Investigated in the Different Sectors (#1, #2 and #3) during the Entire Study.

	Urban (U)			Urban Background (UB)		
<i>Inorganic Fraction</i>						
	PM ₁₀ vs. PM _{2.5}			PM ₁₀ vs. PM _{2.5}		
	#1	#2	#3	#1	#2	#3
Metals	0.223	0.296	0.652	0.187	0.096	0.616
	PM ₁₀			PM _{2.5}		
	#1 vs. #2	#1 vs. #3	#2 vs. #3	#1 vs. #2	#1 vs. #3	#2 vs. #3
Metals	0.994	0.999	0.998	0.994	0.964	0.987
Metals	0.963	0.616	0.754	0.985	0.716	0.605
<i>Organic Fraction</i>						
	PM ₁₀ vs. PM _{2.5}			PM ₁₀ vs. PM _{2.5}		
	#1	#2	#3	#1	#2	#3
PAHs	0.999	0.880	0.881	0.533	−0.049	0.813
PCCD/Fs	0.951	0.984	0.820	0.941	0.523	0.928
PCBs	0.986	0.945	0.949	0.878	0.927	0.945
All Data	0.987	0.952	0.956	0.896	0.925	0.948
	PM ₁₀			PM _{2.5}		
	#1 vs. #2	#1 vs. #3	#2 vs. #3	#1 vs. #2	#1 vs. #3	#2 vs. #3
PAHs	0.901	0.834	0.837	−0.050	0.953	−0.120
PCCD/Fs	0.958	0.869	0.755	0.875	0.946	0.936
PCBs	0.996	0.993	0.993	0.995	0.999	0.999
All Data	0.996	0.997	0.993	0.982	0.991	0.987
	PM _{2.5}			PM _{2.5}		
	#1 vs. #2	#1 vs. #3	#2 vs. #3	#1 vs. #2	#1 vs. #3	#2 vs. #3
PAHs	0.999	0.980	0.981	0.999	0.917	0.900
PCCD/Fs	0.985	0.955	0.975	0.614	0.872	0.401
PCBs	0.969	0.995	0.995	0.998	0.998	0.998
All Data	0.973	0.962	0.995	0.998	0.992	0.990

As it can be seen, for the inorganic fraction, that is, metals, the correlation coefficients between PM_{10} versus $PM_{2.5}$ in the sectors #1 and #2 are poor whereas they improve over 0.6 in sector #3 of both sites. The low r in #1 and #2 shows different contributions affecting the metals levels over the coal-fired power plant (#1) or the port (#2); on the other hand, the good correlation coefficients found in #3 of both sites (sector #3: wind blows from all other directions) mean that the eventual metals emitted by these two anthropogenic sources do not contribute to their level. Similar considerations can be drawn for the organic fraction. Particularly, it is interesting the correlation coefficients between PAHs—they are very good for the urban site (U) ranging between 0.999 (#1) and 0.88 (#2 and #3) whereas they are poor in Urban Background (UB) ranging between -0.049 (#2) and 0.813 (#3). This is another confirmation about the important role played by the coal-fired power plant (sector #1) in the air quality of such urban area as well as the other directions confirm to affect the suburban area.

For better evidencing the correlations among the sectors, a chemometric approach was applied to overall the data by the use of the Tanagra open-source software [73], by means of the centroid merge method and the Euclidean distance as a proximity measure [74,75]. Hierarchical Cluster Analysis (HAC) and Principal Component Analysis (PCA) were used for evidencing eventual similarities.

The HAC shows the presence of three clusters in both sites but the components in the clusters are differently distributed—in particular, in U site cluster #1 is formed by 198 compounds whereas clusters #2 and #3 by 1 (Se and Fluorene, respectively, in $PM_{2.5}$, sector #2, both in fall period); at UB site cluster #1 is formed by three compounds (Naphthalene in $PM_{2.5}$, sectors #1 and #2, in winter period; Cu in $PM_{2.5}$, sector #1, in fall period) and cluster #3 by 2 (Naphthalene in PM_{10} , sector #2, in winter; Naphthalene in PM_{10} , sector #2, in fall) whereas cluster #2 by 195 components. Because the dendrograms are not so explicative, the authors would like to show the PCA representations and the correlation scatterplots—two variables are able to explain almost 85% of the entire dataset. This occurrence is a confirmation about the high correlation in the data and the effectiveness of the samplings performed. Figure 10 shows the PCA (a) and the correlation scatterplot (b) obtained analyzing the data collected at urban site and the PCA (c) and the correlation scatterplot (d) obtained analyzing the data collected at suburban site.

The PCA plots (Figure 10a,c) evidence how the clusters are formed. They appear different according to the locations. The information about Fluorene and Naphthalene is quite important—it confirms the source apportionment to their levels due to the presence of the large port in the investigated area. Likewise, Figure 10b,d is also explicative—the PM_{10} and $PM_{2.5}$ samples groups in similar ways in both cases but preferring opposite axes.

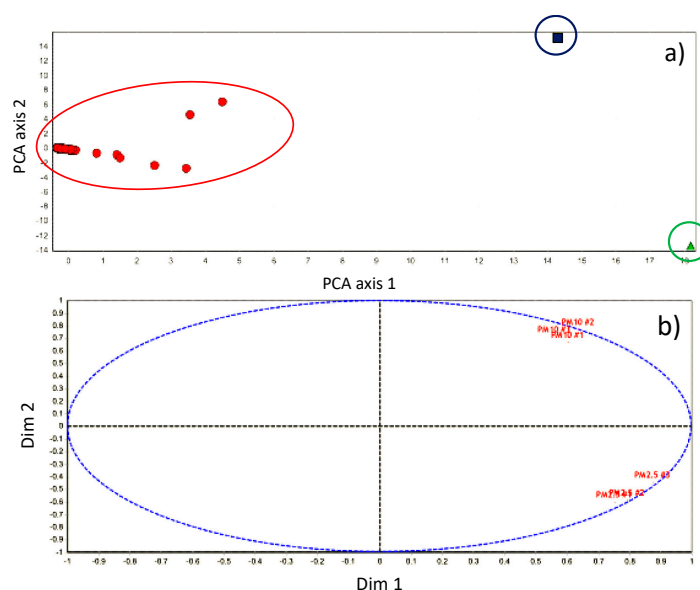


Figure 10. Cont.

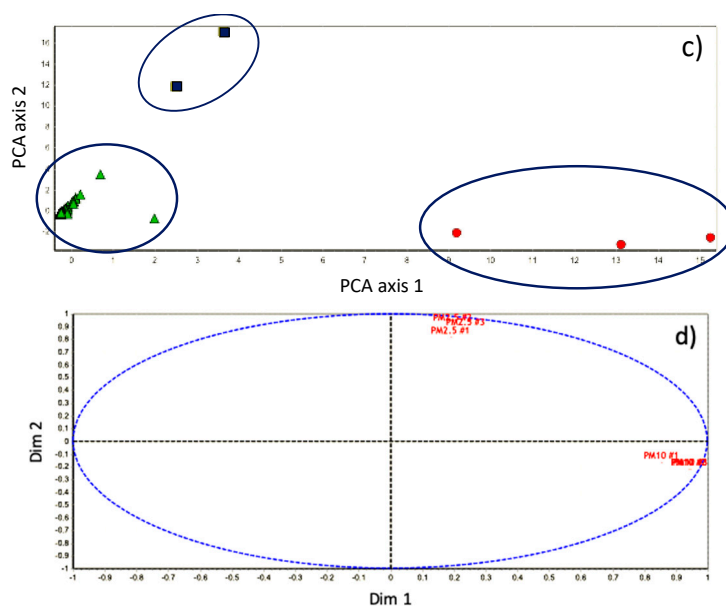


Figure 10. Main results of the chemometric approach to overall the data—Principal Component Analysis (PCA) (a) and correlation scatter (b) plots obtained in downtown Civitavecchia, U; PCA (c) and correlation scatter (d) plots obtained in sampling at the suburban area, UB (red: cluster #1; green: cluster #2; blue: cluster #3).

4. Conclusions

The study performed in the Civitavecchia area has been aimed at highlighting the behavior of pollutants of hygienic-sanitary interest, such as organic contaminants (PCDD/Fs, PCBs and PAHs) and inorganic pollutants such as heavy metals, attributable to the emission sources present in the area. This occurrence has allowed to understand if these pollutants could represent a human health risk for the resident populations and to recommend the most effective risk reduction and mitigation actions.

This paper is based on well-known analytical approaches, the novelty lies in where the different procedures were applied and the relative considerations drawn after them. A good analytical approach, such as performed in this study, is the first step for a correct source apportionment, especially in a very complex area such as Civitavecchia where different contributions affect the air quality, for example, power plant, harbor, autovehicular traffic, domestic heating and so forth. For achieving an accurate source apportionment methodology aimed to understand the real contribution of each source to the air quality, wind selection devices have proven to be effective in achieving this goal, also coupled with a more accurate statistical analysis of the analytical results achieved. This is an uncommon sampling choice (rare, as defined in the introduction) but it has proven itself useful in this approach, few papers are based on this methodology. GC-MS and ICP-MS procedures according to the European directive and guidelines for determining organic and inorganic fractions allowed to investigate 59 species (19 metals, 21 PAHs, 17 PCDD/Fs and 12 PCBs), a chemometric analysis (HAC and PCA) was used for identifying the main compounds responsible in the human exposure. Some doubts, some uncertainty considerations are still present but they can be overcome by planning studies for a longer period of time. The important point which the authors would like to emphasize, is that, beyond the results obtained, the entire methodology (from sampling to the data processing and results evaluation) can be exported in similar environmental studies.

Supplementary Materials: The following are available online at <http://www.mdpi.com/2073-4433/11/1/94/s1>, Tables S1–S8: Table S1. Metal concentrations in PM₁₀ and PM_{2.5} fractions sampled in downtown; Table S2. Metal concentrations in PM₁₀ and PM_{2.5} fractions sampled in suburban area.; Table S3. PAH concentrations in PM₁₀ and PM_{2.5} fraction sampled in downtown; Table S4. PAH concentrations in PM₁₀ and PM_{2.5} fraction sampled in suburban area; Table S5. PCDD/Fs concentrations PM₁₀ and PM_{2.5} fraction sampled in downtown; Table S6. PCDD/Fs concentrations PM₁₀ and PM_{2.5} fraction sampled in suburban area; Table S7. DL-PCBs concentrations

PM₁₀ and PM_{2.5} fraction sampled in downtown; Table S8. DL-PCBs concentrations PM₁₀ and PM_{2.5} fraction sampled in suburban area.

Author Contributions: Conceptualization, M.E.S., G.M. and P.A.; methodology, G.M. and G.C.; software, M.I.; validation, M.I., G.S. and R.V.G.; formal analysis, M.I.; investigation, M.I. and G.S.; resources, G.S.; data curation, M.E.S., I.N. and R.V.G.; writing-original draft preparation, P.A.; writing-review and editing, M.E.S. and P.A.; visualization, G.S.; supervision, G.M. and M.E.S.; project administration, G.S.; funding acquisition, G.M. All authors have read and agreed to the published version of the manuscript.

Funding: This research was performed under the agreement between the Italian Institute of Health (ISS) and the Consortium for the Management of the Environmental Observatory of Civitavecchia, for the realization of a research program having as objective “The evaluation of the levels of organic and inorganic micropollutants in the area of the municipalities of Civitavecchia, Tolfa, Allumiere, Santa Marinella, Monte Romano and Tarquinia affected by emissions from the ENEL thermoelectric power station of Torrevaldaliga North”.

Conflicts of Interest: The authors declare no conflict of interest.

References

1. International Maritime Organization. Third IMO GHG Study 2014. Available online: <http://www.imo.org/en/OurWork/Environment/PollutionPrevention/AirPollution/Documents/Third%20Greenhouse%20Gas%20Study/GHG3%20Executive%20Summary%20and%20Report.pdf> (accessed on 16 September 2019).
2. Legislative Decree 155/10. Attuazione della direttiva 2008/50/CE relativa alla qualità dell’aria ambiente e per un’aria più pulita in Europa. *Gazz. Uff.* **2010**, *216*, 1–111.
3. Eyring, V.; Köhler, H.W.; van Ardenne, J.; Lauer, A. Emissions from international shipping: 1. The last 50 years. *J. Geophys. Res.* **2005**, *110*, D17305. [[CrossRef](#)]
4. Song, S. Ship emissions inventory, social cost and eco-efficiency in Shanghai Yangshan port. *Atmos. Environ.* **2014**, *82*, 288–297. [[CrossRef](#)]
5. Merico, E.; Donato, A.; Gambaro, A.; Cesari, D.; Gregoris, E.; Barbaro, E.; Dinoi, A.; Giovanelli, G.; Masieri, S.; Contini, D. Influence of in-port ships emissions to gaseous atmospheric pollutants and to particulate matter of different sizes in a Mediterranean harbour in Italy. *Atmos. Environ.* **2016**, *139*, 1–10. [[CrossRef](#)]
6. Murena, F.; Mocerino, L.; Quaranta, F.; Toscano, D. Impact on air quality of cruise ship emissions in Naples, Italy. *Atmos. Environ.* **2018**, *187*, 70–83. [[CrossRef](#)]
7. Tzannatos, E. Ship emissions and their externalities for the port of Piraeus-Greece. *Atmos. Environ.* **2010**, *44*, 400–407. [[CrossRef](#)]
8. Pérez, N.; Pey, J.; Reche, C.; Joaquim Cortés, J.; Alastuey, A.; Querol, X. Impact of harbour emissions on ambient PM₁₀ and PM_{2.5} in Barcelona (Spain): Evidences of secondary aerosol formation within the urban area. *Sci. Total Environ.* **2016**, *571*, 237–250. [[CrossRef](#)]
9. Gariazzo, C.; Papaleo, V.; Pelliccioni, A.; Calori, G.; Radice, P.; Tinarelli, G. Application of a Lagrangian particle model to assess the impact of harbour, industrial and urban activities on air quality in the Taranto area, Italy. *Atmos. Environ.* **2007**, *41*, 6432–6444. [[CrossRef](#)]
10. Viana, M.; Hammingh, P.; Colette, A.; Querol, X.; Degraeuwe, B.; de Vlieger, I.; van Aardenne, J. Impact of maritime transport emissions on coastal air quality in Europe. *Atmos. Environ.* **2014**, *90*, 96–105. [[CrossRef](#)]
11. Adamo, F.; Andria, G.; Cavone, G.; De Capua, C.; Lanzolla, A.; Morello, R.; Spadavecchia, M. Estimation of ship emissions in the port of Taranto. *Measurement* **2014**, *14*, 982–988. [[CrossRef](#)]
12. Prati, M.V.; Costagliola, M.A.; Quaranta, F.; Murena, F. Assessment of ambient air quality in the port of Naples. *J. Air Waste Manag.* **2015**, *65*, 970–979. [[CrossRef](#)] [[PubMed](#)]
13. Mamoudou, I.; Zhang, F.; Chen, Q.; Wang, P.; Chen, Y. Characteristics of PM_{2.5} from ship emissions and their impacts on the ambient air: A case study in Yangshan Harbor, Shanghai. *Sci. Total Environ.* **2018**, *640–641*, 207–216. [[CrossRef](#)] [[PubMed](#)]
14. Ault, A.P.; Moore, M.J.; Furutani, H.; Prather, K.A. Impact of emissions from the Los Angeles port region on San Diego air quality during regional transport events. *Environ. Sci. Technol.* **2009**, *43*, 3500–3506. [[CrossRef](#)] [[PubMed](#)]

15. Avino, P.; De Lisio, V.; Grassi, M.; Lucchetta, M.C.; Messina, B.; Monaco, G.; Petracchia, L.; Quartieri, G.; Rosentzweig, R.; Russo, M.V.; et al. Influence of air pollution on chronic obstructive respiratory diseases: Comparison between city (Rome) and hillcountry environments and climates. *Ann. Chim.* **2004**, *94*, 629–635. [[CrossRef](#)] [[PubMed](#)]
16. Fano, V.; Michelozzi, P.; Ancona, C.; Capon, A.; Forastiere, F.; Perucci, C.A. Occupational and environmental exposures and lung cancer in an industrialised area in Italy. *Occup. Environ. Med.* **2004**, *61*, 757–763. [[CrossRef](#)] [[PubMed](#)]
17. Benedetti, M.; Iavarone, I.; Comba, P. Cancer risk associated with residential proximity to industrial sites: A review. *Arch. Environ. Health* **2001**, *56*, 342–349. [[CrossRef](#)]
18. Fano, V.; Forastiere, F.; Papini, P.; Tancioni, V.; Di Napoli, A.; Perucci, C.A. Mortality and hospital admissions in the industrial area of Civitavecchia, 1997–2004. *Epidemiol. Prev.* **2006**, *30*, 221–226.
19. Ciccone, G.; Forastiere, F.; Agabiti, N.; Biggeri, A.; Bisanti, L.; Chellini, E.; Corbo, G.; Dell’Orco, V.; Dalmasso, P.; Volante, T.F.; et al. Road traffic and adverse respiratory effects in children. SIDRIA Collaborative Group. *Occup. Environ. Med.* **1998**, *55*, 771–778. [[CrossRef](#)]
20. Heinrich, J.; Wichmann, H.E. Traffic related pollutants in Europe and their effect on allergic disease. *Curr. Opin. Allergy Clin. Immunol.* **2004**, *4*, 341–348. [[CrossRef](#)]
21. Schwartz, J. Air pollution and children’s health. *Pediatrics* **2004**, *113*, 1037–1043.
22. Febo, A.; Guglielmi, F.; Manigrasso, M.; Ciambottini, V.; Avino, P. Local air pollution and long-range mass transport of atmospheric particulate matter: A comparative study of the temporal evolution of the aerosol size fractions. *Atmos. Pollut. Res.* **2010**, *1*, 141–146. [[CrossRef](#)]
23. Manigrasso, M.; Febo, A.; Guglielmi, F.; Ciambottini, V.; Avino, P. Relevance of aerosol size spectrum analysis as support to qualitative source apportionment studies. *Environ. Pollut.* **2012**, *170*, 43–51. [[CrossRef](#)] [[PubMed](#)]
24. Merico, E.; Dinoi, A.; Contini, D. Development of an integrated modelling-measurement system for T near-real-time estimates of harbour activity impact to atmospheric pollution in coastal cities. *Transp. Res. D-Transp. Environ.* **2019**, *73*, 108–119. [[CrossRef](#)]
25. Saraga, D.E.; Tolis, E.I.; Maggos, T.; Vasilakos, C.; Bartzis, J.G. PM_{2.5} source apportionment for the port city of Thessaloniki, Greece. *Sci. Total Environ.* **2019**, *650*, 2337–2354. [[CrossRef](#)] [[PubMed](#)]
26. Galarneau, E. Source specificity and atmospheric processing of airborne PAHs: Implications for source apportionment. *Atmos. Environ.* **2008**, *42*, 8139–8149. [[CrossRef](#)]
27. Cecinato, A.; Guerriero, E.; Balducci, C.; Muto, V. Use of the PAH fingerprints for identifying pollution sources. *Urban Clim.* **2014**, *10*, 630–643. [[CrossRef](#)]
28. Khaniabadi, Y.O.; Sicard, P.; Taiwo, A.M.; De Marco, A.; Esmaeili, S.; Rashidi, R. Modeling of particulate matter dispersion from a cement plant: Upwind-downwind case study. *J. Environ. Chem. Eng.* **2018**, *6*, 3104–3110. [[CrossRef](#)]
29. Avino, P.; Capannesi, G.; Rosada, A. Heavy metal determination in atmospheric particulate matter by Instrumental Neutron Activation Analysis. *Microchem. J.* **2008**, *88*, 97–106. [[CrossRef](#)]
30. Manigrasso, M.; Abballe, F.; Jack, R.F.; Avino, P. Time-resolved measurement of the ionic fraction of atmospheric fine particulate matter. *J. Chromatogr. Sci.* **2010**, *48*, 549–552. [[CrossRef](#)]
31. Stabile, L.; Buonanno, G.; Avino, P.; Fuoco, F.C. Dimensional and chemical characterization of airborne particles in schools: Respiratory effects in children. *Aerosol Air Qual. Res.* **2013**, *13*, 887–900. [[CrossRef](#)]
32. Alleman, L.Y.; Lamaison, L.; Perdrix, E.; Robache, A.; Galloo, J.C. PM₁₀ metal concentrations and source identification using positive matrix factorization and wind sectoring in a French industrial zone. *Atmos. Res.* **2010**, *96*, 612–625. [[CrossRef](#)]
33. Martínez, K.; Austrui, J.R.; Jover, E.; Abalos, M.; Rivera, J.; Abad, E. Assessment of the emission of PCDD/Fs and dioxin-like PCBs from an industrial area over a nearby town using a selective wind direction sampling device. *Environ. Pollut.* **2010**, *158*, 764–769. [[CrossRef](#)] [[PubMed](#)]
34. Venturini, E.; Vassura, I.; Raffo, S.; Ferroni, L.; Bernardi, E.; Passarini, F. Source apportionment and location by selective wind sampling and Positive Matrix Factorization. *Environ. Sci. Pollut. Res.* **2014**, *21*, 11634–11648. [[CrossRef](#)] [[PubMed](#)]
35. Venturini, E.; Vassura, I.; Passarini, F.; Morselli, L. Source apportionment study based on selective wind direction sampling. *Environ. Eng. Manag. J.* **2013**, *12*, 233–236.

36. Avino, P.; Carconi, P.L.; Lepore, L.; Moauro, A. Nutritional and environmental properties of algal products used in healthy diet by INAA and ICP-AES. *J. Radioanal. Nucl. Chem.* **2000**, *244*, 247–252. [[CrossRef](#)]
37. Settimo, G.; Viviano, G. Atmospheric depositions of persistent pollutants: Methodological aspects and values from case studies. *Ann. Ist. Super. Sanita* **2015**, *51*, 298–304.
38. Avino, P.; Manigrasso, M. Ten-year measurements of gaseous pollutants in urban air by an open-path analyzer. *Atmos. Environ.* **2008**, *42*, 4138–4148. [[CrossRef](#)]
39. Avino, P.; Capannesi, G.; Rosada, A. Ultra-trace nutritional and toxicological elements in Rome and Florence drinking waters determined by Instrumental Neutron Activation Analysis. *Microchem. J.* **2011**, *97*, 144–153. [[CrossRef](#)]
40. Di Vaio, P.; Magli, E.; Barbato, F.; Caliendo, G.; Cocozziello, B.; Corvino, A.; De Marco, A.; Fiorino, F.; Frecentese, F.; Onorati, G.; et al. Chemical composition of PM₁₀ at urban sites in Naples (Italy). *Atmosphere* **2016**, *7*, 163. [[CrossRef](#)]
41. Di Vaio, P.; Cocozziello, B.; Corvino, A.; Fiorino, F.; Frecentese, F.; Magli, E.; Onorati, G.; Saccone, I.; Santagada, V.; Settimo, G.; et al. Level, potential sources of polycyclic aromatic hydrocarbons (PAHs) in particulate matter (PM₁₀) in Naples. *Atmos. Environ.* **2016**, *129*, 186–196. [[CrossRef](#)]
42. Avino, P.; Brocco, D.; Lepore, L.; Pareti, S. Interpretation of atmospheric pollution phenomena in relationship with the vertical atmospheric remixing by means of natural radioactivity measurements (radon) of particulate matter. *Ann. Chim.-Rome* **2003**, *93*, 589–594.
43. Manigrasso, M.; Avino, P. Fast evolution of urban ultrafine particles: Implications for deposition doses in the human respiratory system. *Atmos. Environ.* **2002**, *51*, 116–123. [[CrossRef](#)]
44. Avino, P.; Capannesi, G.; Rosada, A. Characterization and distribution of mineral content in fine and coarse airborne particle fractions by neutron activation analysis. *Toxicol. Environ. Chem.* **2006**, *88*, 633–647. [[CrossRef](#)]
45. Avino, P.; Manigrasso, M.; Rosada, A.; Dodaro, A. Measurement of organic and elemental carbon in downtown Rome and background area: Physical behavior and chemical speciation. *Environ. Sci. Process. Impacts* **2015**, *17*, 300–315. [[CrossRef](#)] [[PubMed](#)]
46. Khalili, N.R.; Scheff, P.A.; Holsen, T.M. PAH source fingerprints for coke ovens, diesel and gasoline engines, highway tunnels, and wood combustion emissions. *Atmos. Environ.* **1995**, *29*, 533–542. [[CrossRef](#)]
47. Rojas, N.Y.; Milquez, H.A.; Sarmiento, H. Characterizing priority polycyclic aromatic hydrocarbons (PAH) in particulate matter from diesel and palm oil-based biodiesel B15 combustion. *Atmos. Environ.* **2011**, *45*, 6158–6162. [[CrossRef](#)]
48. Yang, X.; Ren, D.; Sun, W.; Li, X.; Huang, B.; Chen, R.; Lin, C.; Pan, X. Polycyclic aromatic hydrocarbons associated with total suspended particles and surface soils in Kunming, China: Distribution, possible sources, and cancer risks. *Environ. Sci. Pollut. Res.* **2015**, *22*, 6696–6712. [[CrossRef](#)]
49. Villanueva, F.; Tapia, A.; Cabañas, B.; Martínez, E.; Albaladejo, J. Characterization of particulate polycyclic aromatic hydrocarbons in an urban atmosphere of central-southern Spain. *Environ. Sci. Pollut. Res.* **2015**, *22*, 18814–18823. [[CrossRef](#)]
50. Lynam, M.M.; Timothy Dvonch, J.; Turlington, J.M.; Olson, D.; Landis, M.S. Combustion-related organic species in temporally resolved urban airborne particulate matter. *Air Qual. Atmos. Hlth.* **2017**, *10*, 917–927. [[CrossRef](#)]
51. Sun, R.-X.; Yang, X.; Li, Q.X.; Wu, Y.-T.; Shao, H.-Y.; Wu, M.-H.; Mai, B.-X. Polycyclic aromatic hydrocarbons in marine organisms from Mischief Reef in the South China sea: Implications for sources and human exposure. *Mar. Pollut. Bull.* **2019**, *149*, 110623. [[CrossRef](#)]
52. Wang, C.; Meng, Z.; Yao, P.; Zhang, L.; Wang, Z.; Lv, Y.; Tian, Y.; Feng, Y. Sources-specific carcinogenicity and mutagenicity of PM_{2.5}-bound PAHs in Beijing, China: Variations of contributions under diverse anthropogenic activities. *Ecotoxicol. Environ. Saf.* **2019**, *183*, 109552. [[CrossRef](#)] [[PubMed](#)]
53. Llamas, A.; Al-Lal, A.-M.; García-Martínez, M.-J.; Ortega, M.F.; Llamas, J.F.; Lapuerta, M.; Canoira, L. Polycyclic Aromatic Hydrocarbons (PAHs) produced in the combustion of fatty acid alkyl esters from different feedstocks: Quantification, statistical analysis and mechanisms of formation. *Sci. Total Environ.* **2017**, *586*, 446–456. [[CrossRef](#)] [[PubMed](#)]
54. Dat, N.-D.; Chang, M.B. Review on characteristics of PAHs in atmosphere, anthropogenic sources and control technologies. *Sci. Total Environ.* **2017**, *609*, 682–693. [[CrossRef](#)] [[PubMed](#)]

55. Kim, S.-J.; Park, M.-K.; Lee, S.-E.; Go, H.-J.; Cho, B.-C.; Lee, Y.-S.; Choi, S.-D. Impact of traffic volumes on levels, patterns, and toxicity of polycyclic aromatic hydrocarbons in roadside soils. *Environ. Sci.-Proc. Imp.* **2019**, *21*, 174–182. [[CrossRef](#)] [[PubMed](#)]
56. Gune, M.M.; Ma, W.-L.; Sampath, S.; Li, W.; Li, Y.-F.; Udayashankar, H.N.; Balakrishna, K.; Zhang, Z. Occurrence of polycyclic aromatic hydrocarbons (PAHs) in air and soil surrounding a coal-fired thermal power plant in the south-west coast of India. *Environ. Sci. Pollut. Res.* **2019**, *26*, 22772–22782. [[CrossRef](#)] [[PubMed](#)]
57. Iakovides, M.; Stephanou, E.G.; Apostolaki, M.; Hadjicharalambous, M.; Evans, J.S.; Koutrakis, P.; Achilleos, S. Study of the occurrence of airborne Polycyclic Aromatic Hydrocarbons associated with respirable particles in two coastal cities at Eastern Mediterranean: Levels, source apportionment, and potential risk for human health. *Atmos. Environ.* **2019**, *213*, 170–184. [[CrossRef](#)]
58. Costabile, F.; Alas, H.; Aufderheide, M.; Avino, P.; Amato, F.; Argentini, S.; Barnaba, F.; Berico, M.; Bernardoni, V.; Biondi, R.; et al. First Results of the “Carbonaceous Aerosol in Rome and Environs (CARE)” Experiment: Beyond Current Standards for PM₁₀. *Atmosphere* **2017**, *8*, 249. [[CrossRef](#)]
59. Miura, K.; Shimada, K.; Sugiyama, T.; Sato, K.; Takami, A.; Chan, C.K.; Kim, I.S.; Kim, Y.P.; Lin, N.-H.; Hatakeyama, S. Seasonal and annual changes in PAH concentrations in a remote site in the Pacific Ocean. *Sci. Rep.-UK* **2019**, *9*, 12591. [[CrossRef](#)]
60. Lu, C.M.; Dat, N.D.; Lien, C.K.; Chi, K.H.; Chang, M.B. Characteristics of fine particulate matter and Polycyclic Aromatic Hydrocarbons emitted from coal combustion processes. *Energ. Fuels* **2019**, *33*, 10247–10254. [[CrossRef](#)]
61. Sazykin, I.S.; Minkina, T.M.; Grigoryeva, T.V.; Khmelevtsova, L.E.; Sushkova, S.N.; Laikov, A.V.; Antonenko, E.M.; Ismagilova, R.K.; Seliverstova, E.Y.; Mandzhieva, S.S.; et al. PAHs distribution and cultivable PAHs degraders’ biodiversity in soils and surface sediments of the impact zone of the Novocheerkassk thermal electric power plant (Russia). *Environ. Earth Sci.* **2019**, *78*, 581. [[CrossRef](#)]
62. Diesch, J.-M.; Drewnick, F.; Klimach, T.; Borrmann, S. Investigation of gaseous and particulate emissions from various marine vessel types measured on the banks of the Elbe in Northern Germany. *Atmos. Chem. Phys.* **2013**, *13*, 3603–3618. [[CrossRef](#)]
63. Czech, H.; Stengel, B.; Adam, T.; Sklorz, M.; Streibel, T.; Zimmermann, R. A chemometric investigation of aromatic emission profiles from a marine engine in comparison with residential wood combustion and road traffic: Implications for source apportionment inside and outside sulphur emission control areas. *Atmos. Environ.* **2017**, *167*, 212–222. [[CrossRef](#)]
64. Zhao, J.; Zhang, Y.; Wang, T.; Sun, L.; Yang, Z.; Lin, Y.; Chen, Y.; Mao, H. Characterization of PM_{2.5}-bound polycyclic aromatic hydrocarbons and their derivatives (nitro-and oxy-PAHs) emissions from two ship engines under different operating conditions. *Chemosphere* **2019**, *225*, 43–52. [[CrossRef](#)] [[PubMed](#)]
65. Pereira, G.M.; Oraggio, B.; Teinilä, K.; Custódio, D.; Huang, X.; Hillamo, R.; Alves, C.A.; Balasubramanian, R.; Rojas, N.Y.; Sanchez-Ccoyllo, O.R.; et al. A comparative chemical study of PM₁₀ in three Latin American cities: Lima, Medellín, and São Paulo. *Air Qual. Atmos. Health* **2019**, *12*, 1141–1152. [[CrossRef](#)]
66. Jia, C.; Batterman, S. A critical review of naphthalene sources and exposures relevant to indoor and outdoor air. *Int. J. Environ. Res. Public Health* **2010**, *7*, 2903–2939. [[CrossRef](#)]
67. Batterman, S.; Chin, J.-Y.; Jia, C.; Godwin, C.; Parker, E.; Robins, T.; Max, P.; Lewis, T. Sources, concentrations and risks of naphthalene in indoor and outdoor air. *Indoor Air* **2012**, *22*, 266–278. [[CrossRef](#)]
68. Li, X.; Li, Y.; Zhang, Q.; Wang, P.; Yang, H.; Jiang, G.; Wei, F. Evaluation of atmospheric sources of PCDD/Fs, PCBs and PBDEs around a steel industrial complex in northeast China using passive air samplers. *Chemosphere* **2011**, *84*, 957–963. [[CrossRef](#)]
69. Chen, T.; Zhan, M.-X.; Lin, X.-Q.; Fu, J.-Y.; Lu, S.-Y.; Li, X.-D. Distribution of PCDD/Fs in the fly ash and atmospheric air of two typical hazardous waste incinerators in eastern China. *Environ. Sci. Pollut. Res.* **2014**, *22*, 1207–1214. [[CrossRef](#)]
70. Paradiz, B.; Dilara, P.; Umlauf, G.; Bajsic, I.; Butala, V. Dioxin emissions from coal combustion in domestic stove: Formation in the chimney and coal chlorine content influence. *Therm. Sci.* **2015**, *19*, 295–304. [[CrossRef](#)]
71. Huber, F.; Herzel, H.; Adam, C.; Mallow, O.; Blasenbauer, D.; Fellner, J. Combined disc pelletisation and thermal treatment of MSWI fly ash. *Waste Manag.* **2018**, *73*, 381–391. [[CrossRef](#)]

72. Zhang, G.; Huang, X.; Liao, W.; Kang, S.; Ren, M.; Hai, J. Measurement of dioxin emissions from a small-scale waste incinerator in the absence of air pollution controls. *Int. J. Env. Res. Pub. Health* **2019**, *16*, 1267. [[CrossRef](#)] [[PubMed](#)]
73. Tanagra. Available online: <https://eric.univ-lyon2.fr/~ricco/tanagra/en/tanagra.html> (accessed on 10 October 2019).
74. Avino, P.; Capannesi, G.; Manigrasso, M.; Sabbioni, E.; Rosada, A. Element assessment in whole blood, serum and urine of three Italian healthy sub-populations by INAA. *Microchem. J.* **2011**, *99*, 548–555. [[CrossRef](#)]
75. Avino, P.; Capannesi, G.; Renzi, L.; Rosada, A. Instrumental neutron activation analysis and statistical approach for determining baseline values of essential and toxic elements in hairs of high school students. *Ecotoxicol. Environ. Saf.* **2013**, *92*, 206–214. [[CrossRef](#)] [[PubMed](#)]



© 2020 by the authors. Licensee MDPI, Basel, Switzerland. This article is an open access article distributed under the terms and conditions of the Creative Commons Attribution (CC BY) license (<http://creativecommons.org/licenses/by/4.0/>).